Ninth International Conference on CFD in the Minerals and Process Industries
CSIRO, Melbourne, Australia
10-12 December 2012

PREDICTING SURFACE PROFILE EVOLUTION CAUSED BY SOLID PARTICLE EROSION

Christopher B. SOLNORDAL[1*] and Chong Y. WONG[2]

[1] CSIRO Mathematics, Informatics and Statistics, Clayton, Victoria 3169, AUSTRALIA
[2] CSIRO Process Science and Engineering, Highett, Victoria 3169, AUSTRALIA
*Corresponding author, E-mail address: chris.solnordal@csiro.au

ABSTRACT

Erosion of surfaces by particle impact correlates with the velocity and approach angle of the impacting particle. As a surface erodes, its profile changes, and this evolving profile affects the approach conditions of particles and hence the local erosion rate of the surface. The coupling between surface profile and erosion rate of the profile can be highly unstable and in industrial situations may lead to pitting or holing of the surface and catastrophic failure.

This paper presents a numerical analysis of surface evolution due to erosion by sand particles suspended in air. The profiles investigated include a cylindrical rod and a flat plate with sharp edged hole. CFD is used to predict flow and particle dynamics on and around these surfaces, while a simplified two-dimensional model that assumes high Stokes number is then used to investigate profile evolution. It is found that standard erosion rate equations can predict profile evolution of a cylindrical rod to within ±6% of experimental data. However, erosion near a sharp edge requires additional assumptions to allow good prediction, and a number of options are presented. Ultimately, such equations can be included within the moving mesh capability of a CFD solver to predict this transient behaviour.

NOMENCLATURE

A,B adjustable parameters in Eq. (2)
e specific erosion rate, kg kg^{-1}
$f(\alpha)$ function expressed in Eq. (2)
i specific segment number for particle-only model. Used as a subscript to denote a value related to that segment.
K adjustable parameter in Eq. (1)
$\dot{m}$ mass impact rate, kg s^{-1} m^{2}
n exponent in Eq. (1)
$\boldsymbol{S}$ displacement vector of segment, m
t time, s
V impact velocity, m s^{-1}
W,X,Y,Z adjustable parameters in Eq. (2)
y, z co-ordinate system, m

α impact angle, °
φ limit angle in Eq. (2), °
θ angle of surface segment, °
ρ_s density of surface, kg m^{-3}

INTRODUCTION

It is well established initially by Finnie (Finnie, 1960) that solid particle erosion rate (e) is governed by the particle impact velocity (V), particle impact angle (α), particle shape, and many material properties of both the impacting particle and the target surface. The relationship between these parameters is shown in Eq. (1), where K and n are constants specific to a given particle/surface combination, and f(α) is some function that again is specific for a given particle and surface.

$$e = KV^n f(\alpha) \tag{1}$$

The use of CFD in modelling of erosion so far has been limited to using Eq. (1) or variants thereof to predict the local surface erosion rate for a given geometry. However, as a surface erodes, the profile of the surface changes, and this in turn affects the impact angle and velocity, and hence the local erosion rate.

The authors have previously shown (Solnordal and Wong, 2011; Wong *et al.*, 2012) that by using CFD to predict the erosion rate around a single hole in a flat plate, the evolution of planar regions of the surface can be determined. However, where there is an abrupt change in surface direction (such as at a sharp edge) it is not clear how the surface can be predicted to evolve.

In this work we present some simplified analyses of this problem, considering two surface geometries. The first is the surface of a cylinder in cross-flow, while the second is the aforementioned hole in a flat plate. Erosion distributions on these geometries are predicted using CFD and are compared under a number of conditions. Results are used to justify creating a simplified particle-only model of the systems that can update the surface geometry based on the local predicted erosion rate. The simplified model is then used to investigate different ways of analysing the surface data.

CFD MODEL

Modelling Approach

The commercial CFD code ANSYS-CFX13 was used to perform an Eulerian-Lagrangian analysis of air/solid particle flow through the flow domain. The standard Navier-Stokes equations were solved for the Eulerian phase, while Lagrangian analysis of particles was used to determine particle paths as a post-processing step. This approach was valid as the particle phase was very dilute,

having a particle volume fraction of less than 10^{-4}. Further details of the equations and approach are published elsewhere (ANSYS, 2010; Wong *et al.*, 2012).

Geometry and Mesh

Two geometries were used in the CFD analysis. The first one is shown in Figure 1, and represents the experimental rig that was used to perform erosion rate analyses for the work. The geometry extended from the point of entry of the solid particles, through the test section, and approximately 1 m downstream of the test section. This allowed for the distribution of particles in the test section to be modelled, rather than estimated. An unstructured mesh of 2,750,000 cells was superimposed, using mesh inflation adjacent to walls. A higher concentration of cells was used around the test section in order to capture the flow field in that region accurately.

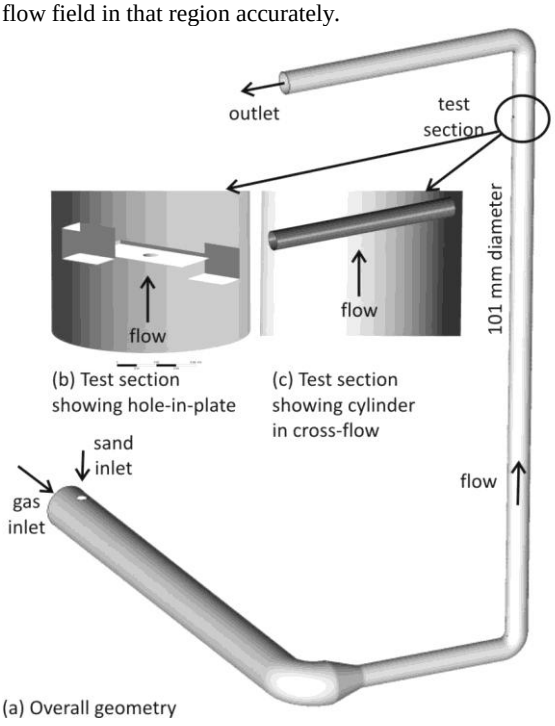

Figure 1: (a) Overall geometry; (b) Hole-in-plate detail; (c) cylinder detail.

A less extensive geometry was also used to analyse the erosion rate on and around the test section itself. This reduced geometry is shown in Figure 2, and utilized a hexahedral mesh to capture the detail of both the cylinder and the hole-in-plate test section. The profile of the hole was determined using measurements of it in an uneroded state, and then also after exposure to 50 kg of erodent (Figure 3).

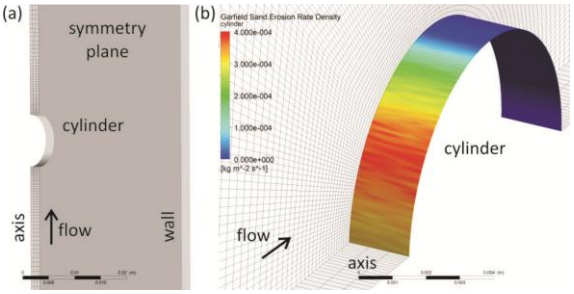

Figure 2: (a) Quasi-two-dimensional geometry of cylinder-in-pipe; (b) predicted erosion distribution.

Materials, Boundary Conditions and Solution Strategy

The materials of interest in the current work are aluminium and silica sand. The sand was relatively coarse, with a median diameter of 223 μm. It was fed into the flow domain at a rate of 0.030 kg s^{-1}. The test sections (both cylinder and plate) were made from grade 6061 aluminium. The cylinder had a diameter of 10 mm, while the plate was nominally 2 mm thick, 25 mm wide, and had a bevelled hole of diameter 8 mm centrally located through it. Both specimens were mounted within the 101 mm diameter circular wind tunnel.

The boundary conditions for the model analyses are summarised in Table 1. The air velocity through the test section was 80 m s^{-1}, so the inlet boundary (of larger cross-sectional area in the full geometry model, see Figure 1a) was specified to ensure this velocity in the test section, while the inlet turbulence quantities were derived from a specified turbulence intensity of 5%. Particles entered the full geometry model through the solids inlet with vertical velocity of 1 m s^{-1} where they were entrained into the flow. For the reduced geometry shown in Figure 2 and Figure 3, the solids entered at a velocity of 64 m s^{-1} (determined from analysis using the full geometry) and concentrated over a small patch of inlet so the maximum possible tracks would impact the test piece at the region of interest.

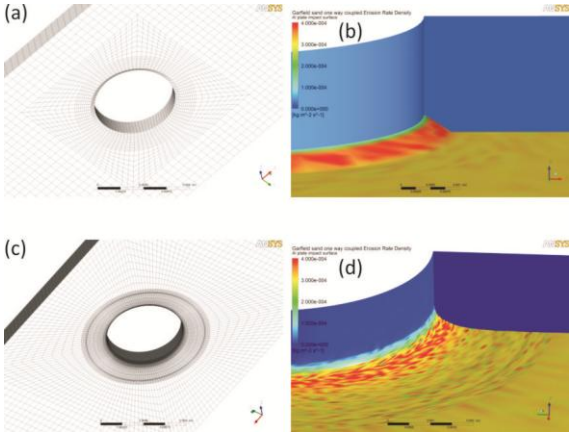

Figure 3: (a) Mesh around hole before erosion; (b) predicted erosion rate before erosion; (c) Mesh around hole with eroded profile; (d) predicted erosion on eroded profile.

Test section mean velocity	Dirichlet	80 m s^{-1}
sand mass flow rate	Dirichlet	0.030 kg s^{-1}
sand inlet velocity	Dirichlet	1 m s^{-1}
outlet	Pressure	0 Pa g
walls	no-slip	

Table 1: Boundary and operating conditions.

K	1.44×10^{-8}	B	5.45	Y	-0.9
n	2.2	W	-3.4	Z	1.556
A	-7	X	0.4	φ	23°

Table 2: Coefficients used in Eq. (1-2) for predicting solid particle erosion caused by sand particles on aluminium.

A simple pressure boundary was used at the outlet, while all walls were specified as no-slip. The k-ε model (Launder and Spalding, 1974) was used to approximate the effects of turbulence, using standard coefficients (Launder and Sharma, 1977).

The Eulerian analyses were performed over several hundred iterations, which led to a well-converged solution of this simple air-only flow. The Lagrangian analysis involved tracking 10^6 particles through the flow domain from the domain entry boundaries. These particles then impacted surfaces in the flow domain, and their impact velocity and angle were used to determine the erosion rate on each cell of the surface. The equation used to determine erosion rate is shown in Eq. (2), and is of the form derived by workers at University of Tulsa (Chen *et al.*, 2004). The coefficients for the equation are shown in Table 2, and were determined using the cylinder in cross-flow method developed by CSIRO (Lester *et al.*, 2010) and utilizing the experimental rig modelled in the current work.

$$f(\alpha) = \begin{cases} A\alpha^2 + B\alpha & \alpha < \varphi \\ X\cos^2\alpha\sin(W\alpha) + Y\sin^2\alpha + Z & \alpha \geq \varphi \end{cases} \quad (2)$$

CFD RESULTS

Figure 2b shows the erosion distribution for the cylinder, while Figure 3b and Figure 3d show that for the hole edge in the uneroded state and after exposure to 50 kg of sand. The cylinder has two bands of maximum erosion on either side of the stagnation point, as has been demonstrated elsewhere (Graham *et al.*, 2009). The uneroded hole edge shows a relatively constant erosion rate on the bevel, with a slightly lower rate on the flat surface of the plate. The erosion rate on the vertical surface of the hole is close to zero, since little material can actually impact this surface, and that which does, does so at a very small angle.

The erosion distribution for the hole edge after 50 kg of sand has passed through the geometry is somewhat different from the uneroded case. This is because the bevelled edge of the hole has been eroded and no longer has sharp changes in angle.

Figure 4 shows the impact rate, impact angle and impact velocity of particles hitting the surface of the cylinder (red dots). Also shown are the theoretical values of these parameters (thick black lines) if all particles were evenly distributed across the flow tunnel cross-section, hit the cylinder in the direction of the flow tunnel axis, and were travelling at the gas velocity of 80 m s^{-1}. There is considerable scatter in the mass impact rate data, due largely to the limitation of tracking only 10^6 particles through the flow domain. A close correspondence exists between the theoretical and predicted impact angle. The impact velocity is relatively constant, but is at a value of 64 m s^{-1}, indicating that the particles have only reached 80% of the free stream gas velocity. These results indicate that the Stokes number of the particles is large enough that the influence of gas streamline curvature on the particle paths can be neglected. It is therefore possible to construct a particle-only model of the two geometries, predict erosion rate on the surface, and use the erosion rate values to update the surface location.

PARTICLE-ONLY MODEL

Modelling Approach

From the findings in Figure 4 it was proposed to develop a two-dimensional particle-only model of the cylinder and hole-in-plate geometries. The cylindrical geometry is used here for the purpose of illustration.

Figure 5 shows two details of the cylinder surface, with y and z-directions defined. The surface of the cylinder was divided initially into 5° line segments (Figure 5a), with typical segments i-1, i and i+1 shown at time t = t_1. Some time later (t = t_2) the surface erodes to the location shown with the dashed lines. Figure 5b shows segments i and i+1 in detail. The angle of segment i is defined by θ_i, and it moves from location A_1B_1 at time t_1, to A_2B_2 at time t_2. It is assumed that the segment moves perpendicular to its surface, in the direction of vector $\mathbf{S_i}$.

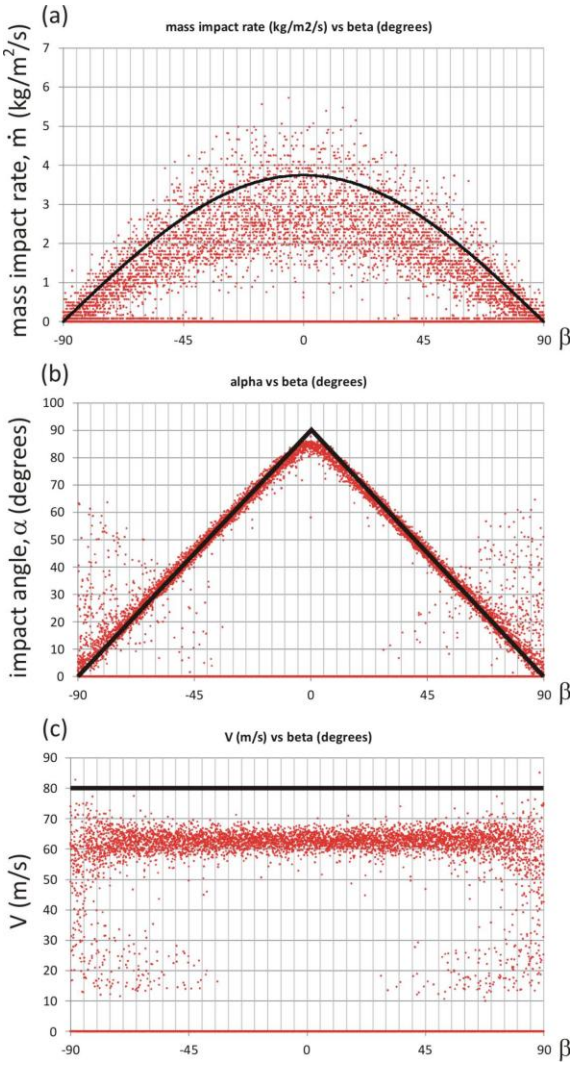

Figure 4: (a) $\dot{m}$, (b) α and (c) V as a function of cylinder angle, β. Red dots = CFD simulation; black line = theoretical values.

It was assumed that the approaching particles were evenly distributed across the pipe with mass rate $\dot{m}$, and that those particles travelled in the -z direction at a velocity of 64 m s^{-1}, as determined from the average impact velocity in Figure 4c. Thus for segment i the angle of impact, α_i, was fully determined by the angle of the segment, θ_i (Figure 5b), as shown in Eq. (3).

$$\alpha_i = \frac{\pi}{2} - \theta_i \quad (3)$$

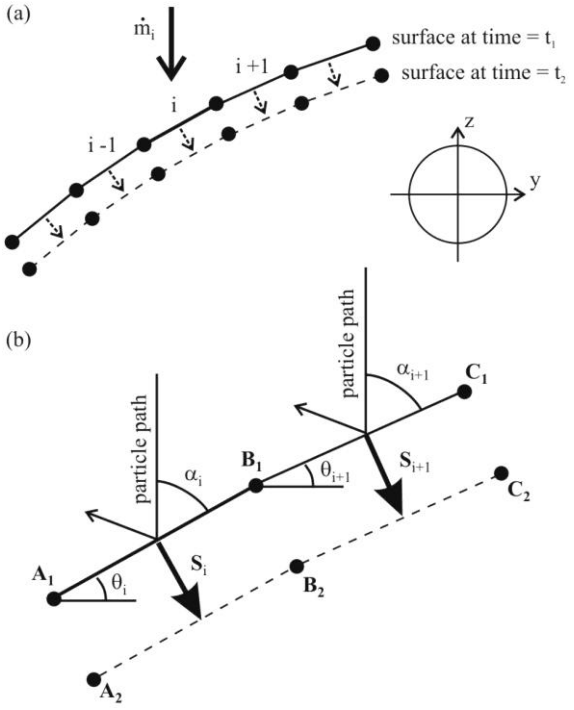

Figure 5: (a) Two-dimensional representation of cylinder surface at time t = t_1 and t = t_2. (b) Segment detail, with parameters defined.

The mass rate of particles impacting segment i, $\dot{m}_i$, was similarly related to the orientation of the segment as shown in Eq. (4).

$$\dot{m}_i = \dot{m}\cos\theta_i \tag{4}$$

The results from the CFD analysis of the full geometry (Figure 4c) showed that particle impact velocities were relatively constant at 64 m s^{-1}, hence

$$U_i = 64 \tag{5}$$

Thus for any given segment i, the parameters α_i, U_i and $\dot{m}_i$ were known, and Eq. (1-2) could be used to calculate the erosion rate for the segment, e_i. The distance the segment moved (ie the depth of eroded surface), $|\mathbf{S_i}|$, was then calculated using Eq. 6.

$$|S_i| = e_i\, \dot{m}_i\, (t_2 - t_1)/\rho_s \tag{6}$$

By calculating each displacement vector $\mathbf{S_i}$, the new location of the segment endpoints A_2, B_2, C_2 (Figure 5b) were calculated by averaging the adjacent displacement vectors, Eq. (7).

$$\overrightarrow{B_1B_2} = 0.5(\vec{S_i} + \overrightarrow{S_{i+1}}) \tag{7}$$

This procedure allowed the full determination of the new surface location. Repeated analyses allowed for successive surface locations to be calculated, thus giving a time-evolved view of the cylinder profile as it was eroded.

The analysis for the hole-in-plate geometry is essentially identical, except that the equation for $\dot{m}_i$ takes into account that the edge profile is that of an axisymmetric hole.

Implementation

Initially the particle-only model was implemented in a spreadsheet. However, to increase the flexibility of the model, it was ported to a stand-alone FORTRAN program.

The model had specific routines that allowed for the number of segments of a surface to be changed based on threshold segment lengths. Thus if over time a surface line segment became too short then adjacent segments could be combined. Similarly, if line segments were too long, they could be divided into smaller segments.

Experimental Data

Experimental data was used for comparison with the model predictions. The hole-in-plate dataset was taken from previously published work by the authors (Wong *et al.*, 2012). A similar dataset was generated using an identical technique for the cylinder geometry, specifically:
-

- Measure cylinder profile using a three-dimensional coordinate measurement machine
- Mount cylinder within experimental wind tunnel
- Pass 50 kg sand particles through the wind tunnel
- Remove cylinder from wind tunnel and re-measure surface profile
- Place cylinder in wind tunnel and pass five additional batches of 50 kg sand particles through the tunnel, measuring the cylinder surface profile after each 50 kg batch.

Detailed explanation of the experimental apparatus and technique is given previously (Wong *et al.*, 2012).

RESULTS FOR PARTICLE-ONLY MODEL

Model Conditions

The model boundary conditions, as modified for a particle-only model, were as specified in Table 1 as used for the full CFD analysis. To optimise the performance of the model, two parameters could be varied, these being the length of each line segment (controlling the spatial resolution) and the time step between calculations (controlling the time resolution).

Cylinder

Initial results of the cylinder model are shown in Figure 6 after passing 100 kg, 200 kg and 300 kg of sand particles through the computational model. The flattening of the surface either side of the centreline is evident, especially at the 300 kg profile. This chevron-like profile is typical of the erosion of a cylinder in cross-flow, and is in keeping with the full CFD predictions shown in Figure 2b. However, the model predicts unrealistic erosion behaviour at extremes of the geometry (y = ±0.005 m), with a cavity predicted to form at this location after 300 kg of erodent has passed through the wind tunnel.

Analysis of the calculation method revealed that the simple assumption used to locate the point B_2, expressed by Eq. (7), was not valid in regions of high curvature or where the model segments were near vertical.

An alternative method for determining the vector $\overrightarrow{B_1B_2}$ and hence the location of point B_2 (Figure 5b) was proposed. Figure 7a reproduces detail of segments i and i+1 as was done in Figure 5b, although in Figure 7a the angle between segments i and i+1 is shown to be larger, and the magnitudes of displacement vectors $\mathbf{S_i}$ and $\mathbf{S_{i+1}}$ are

clearly unequal (as they should be, since the impact angles, and hence erosion rates, are also not equal).

Displacement of segment i (represented by line A_1B_1 in Figure 7) by vector $\mathbf{S_i}$ would sweep out an area represented by the rectangle $R_i = A_1B_1b_{2,i}A_2$ (Figure 7b). Similarly, displacement of segment i+1 by vector $\mathbf{S_{i+1}}$ would sweep out an area represented by rectangle $R_{i+1} = B_1C_1C_2b_{2,i+1}$, also highlighted in Figure 7b.

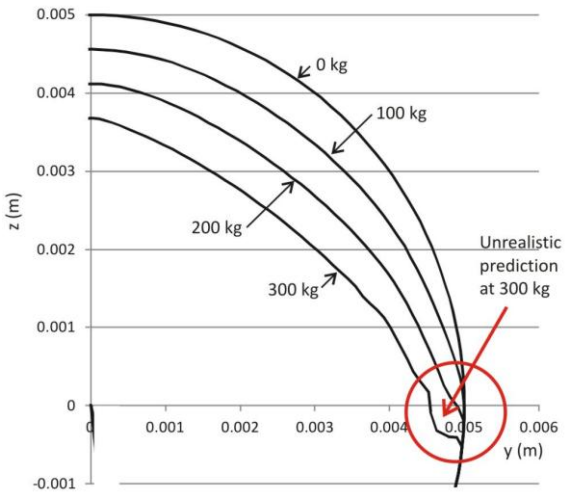

Figure 6: Particle only model initial prediction of cylinder surface evolution.

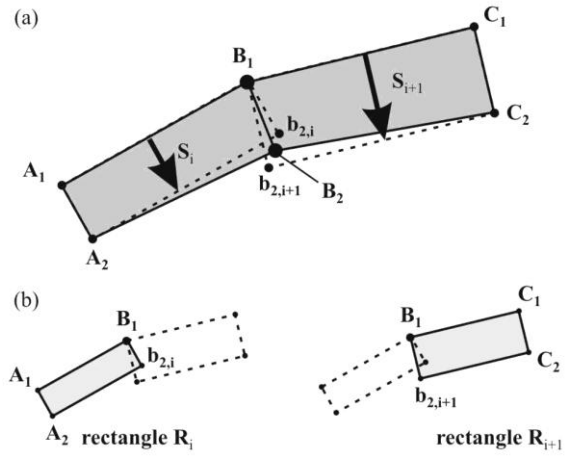

Figure 7: Revised method for determining location of point B_2.

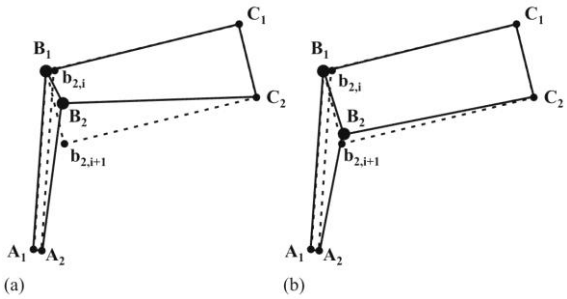

Figure 8: (a) Original method, compared to (b) revised method for determining location of point B_2, using example when section i (A_1B_1) is near vertical.

As before, the direction of $\overrightarrow{B_1B_2}$ was assumed to equal the direction of the sum of vectors $\mathbf{S_i}$ and $\mathbf{S_{i+1}}$. However, its magnitude was determined by assuming the area of shape $A_1B_1C_1C_2B_2A_2$ (grey shading, Figure 7a) was equal to the sum of the areas of R_i and R_{i+1} (grey shading, Figure 7b).

The diagram in Figure 7 does not reveal the subtle difference between the two methods of approach, which is why the prediction in Figure 6 appears reasonable for the majority of the profile. However, consider the case where segment i is near vertical. This is shown in Figure 8, with segment i+1 at a considerably different angle to emphasise the difference. With a near vertical segment, very few particles impact segment i, and they do so at a very small angle. Hence the erosion on that surface is small, the magnitude of vector $\mathbf{S_i}$ is small, and the rectangle R_i is just a thin slither. Using Eq. (7) to locate B_2 would lead to the situation shown in Figure 8a, which tends to increase the sharpness of the angle between segments (compare $A_1B_1C_1$ to $A_2B_2C_2$ in Figure 8a). It is this behaviour that caused the cavity to be predicted (Figure 6). Figure 8b shows the behaviour predicted using the equal-areas method for calculation. Again comparing $A_1B_1C_1$ to $A_2B_2C_2$, it can be seen that the equal–areas method causes a slight flattening off of the profile. This behaviour reflects the experimental data more realistically, as shown in Figure 9. The solids-only model (solid black lines) has slightly over-predicted the experimentally determined chevron-shape of the profile (coloured points). However, the overall shape is very well captured, and the region where the cavity was previously predicted now follows the experimental data closely.

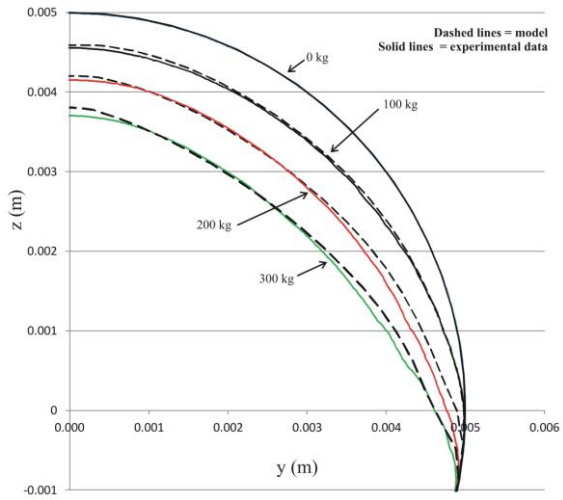

Figure 9: Cylinder profile – Solids-only model prediction using equal-areas approach. points = experimental data; solid lines = model.

Hole-in-Plate

The particle-only erosion model was applied to the edge of the hole for the hole-in-plate geometry, and the results are shown in Figure 10 compared with experimental data (Wong *et al.*, 2012). Figure 10a shows an inset of the plate and hole, where the origin of the y-z coordinate system is defined.

The model over-predicted the experimental data by approximately 15%. Therefore the model predictions were renormalised so that the erosion on the flat surface of the

plate was accurately predicted. This procedure allowed easy comparison of the predicted profile shape with that of the experimental data.

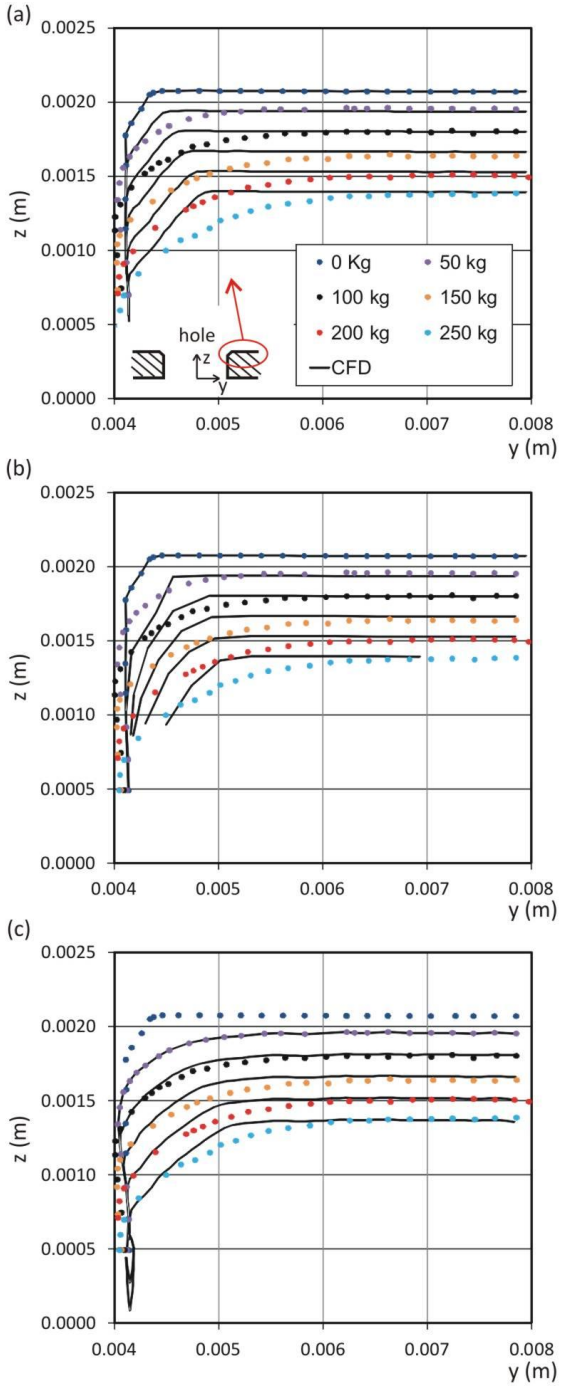

Figure 10: Hole profile – solids only model using equal areas approach. (a) Fine spatial resolution starting with pristine (0 kg) profile; (b) Coarse spatial resolution; (c) Fine spatial resolution starting at 50 kg profile. Model = black lines, experimental data (Wong *et al.*, 2012) shown as points.

The overall rate of erosion was well-predicted on the flat plate surface (due to the renormalisation), but also at the inner surface of the hole. However, the sharp edge between the bevel and the flat plate is not well predicted. The experimental measurements show a rounding off of the surface that extends substantially away from the location of the edge. In contrast the model predicts a surface that remains sharp. Results were not affected by the chosen time step, and the only way of producing a more rounded surface in the model was by *decreasing* the resolution of segments along the surface (Figure 10b), thus causing the effect of adjacent segments to extend further from the edge. This methodology reduced accuracy of the model elsewhere and did not produce particularly good results in the edge region anyway.

The model was re-run using the 50 kg erosion profile as the starting point of the simulation. In this way the initial flattening of the sharp edge had already taken place and so the model did not need to predict this behaviour. The results (Figure 10c) show a significantly improved prediction of the experimental profiles from the flat plate surface right through to the edge of the hole. There is, however, still some under-prediction in the vicinity of y = 0.005 m.

DISCUSSION

Shortcomings of the particle-only model

Inspection of the experimental data in the region of the bevel-flat plate juncture shows that considerably more material is removed from this location than on the surrounding flat surfaces, and this removal leads to the rounding off of the edge. When considering the recognised modes of ductile erosion, there are two mechanisms generally at play. The first of these is the impacting or battering of the surface for impact angles near 90°. The second mechanism is a gouging of material from the surface which is prevalent at acute angles, and is typically maximum at impact angles of 25°-30°. In the current case there are two surfaces, one being impacted by particles at an angle of 90° and the other with impact angles close to 45° (see Figure 11). The combination of particle interactions is leading to removal of surface material beyond what would be expected if only one of the surfaces was present.

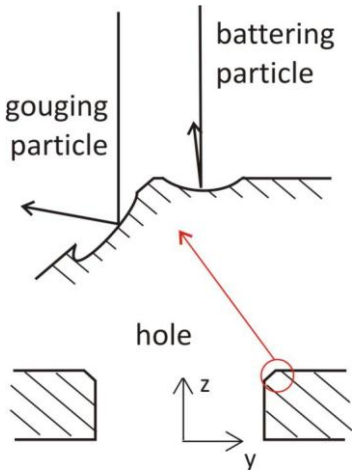

Figure 11: Different erosion mechanisms simultaneously attacking the sharp edge.

Furthermore, individual gouging impacts remove material from a surface *downstream* of the particle impact, rather than perpendicular to the surface. Thus the assumption that erosion occurs perpendicular to a surface may be valid for a large planar surface, but is likely to break down in the region of a sharp edge. It is for this

reason that increasing the resolution of the edge in the particle-only model maintains the sharpness of the edge. The model must ultimately be able to cause movement of the surface element downstream of a particle impact – not just at the surface element itself. Initial attempts to implement such a strategy have so far failed. However, the search for a rational approach to this problem is continuing.

Implementation of the particle-only model within a CFD Framework

The advantage of the particle-only model was that it was possible to update the surface based on the immediate erosion rate. Implementation of this approach within a CFD framework would be time-consuming, but is theoretically possible. It would be necessary to calculate the Eulerian fluid field, then track particles through the flow and use their impact data to determine erosion rates on surfaces in the usual manner. This erosion data would then be used to calculate movement of surface elements, and the mesh updated. The process would then be repeated. The technique would require access to the local erosion rate data to calculate the element displacements. Furthermore, a well-structured mesh would probably be required to enable surface movement without significantly disrupting the mesh.

Naturally it would be preferable to use the largest time step possible in this process, as each re-calculation of the flow and particle field adds to the cost of the simulation. For the current particle-only model simulations of the cylindrical surface, a sensitivity analysis was performed on the time step required to give a time-step-independent solution, and the results are shown in Figure 12. The time step was varied from the value of 5.6 s used in the initial calculations (equivalent to 600 time steps between each profile shown in the Figure) up to 3333.3 s (one time step for each profile). The profiles are shown in Figure 12b, while detailed views of the stagnation point and tangent point are shown in Figure 12a and c. It is seen that a time step a small as 33.3 s is necessary for true time-step-independence. However, a value of 1666.6 s or even 3333.3 s could probably be used depending on the accuracy required.

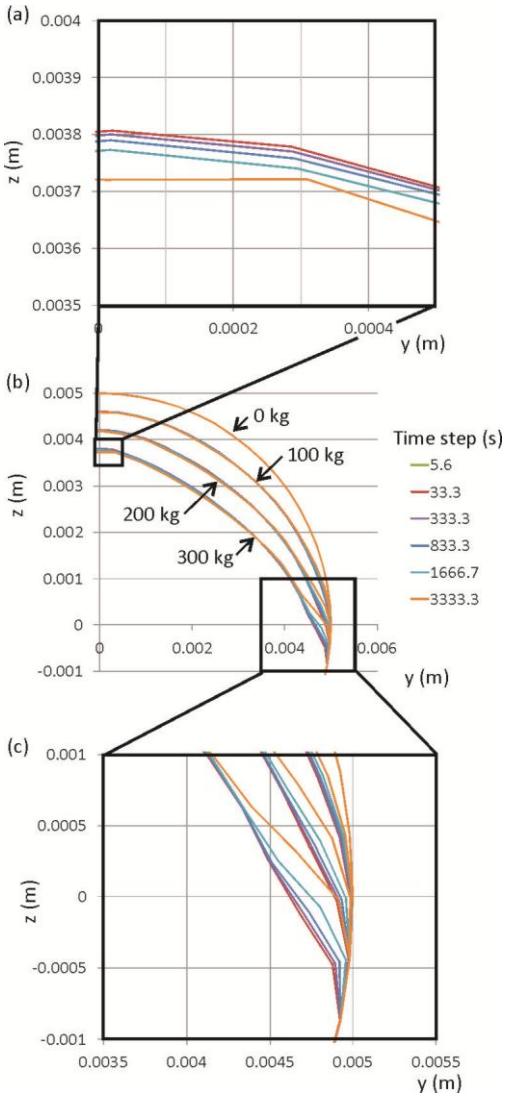

Figure 12: Sensitivity of predicted cylinder profile to time step, (a) detail at stagnation point; (b) full 90° profile, and (c) detail at tangent point.

CONCLUSION

Erosion rate calculations for two geometries – a cylinder, and a plate with central hole – have been reported. A particle-only model of erosion has been implemented as a FORTRAN program to determine the utility of predicting a continually updated surface subject to erosion. It is found that the methodology used can predict smoothly changing surfaces with good accuracy, however, the method fails at sharp edges between planar surfaces. To implement the model within a CFD framework would be costly but achievable. Results suggest that for the conditions studied here, a time step of 33.3 s is necessary to give results independent of time step. However, larger time step values could also be used depending on the accuracy of calculation necessary for a particular application.

REFERENCES

ANSYS, (2010), ANSYS-CFX13.0 User Manual. Canonsburg, PA, USA, ANSYS Inc.

CHEN, X., MCLAURY, B.S. and SHIRAZI, S.A., (2004), "Application and experimental validation of a computational fluid dynamics (CFD)-based erosion prediction model in elbows and plugged tees", *Computers & Fluids* **33**(10): 1251-1272.

FINNIE, I., (1960), "Erosion of surfaces by solid particles", *Wear* **3**(2): 87-103.

GRAHAM, L.J.W., LESTER, D.R. and WU, J., (2009). *"Slurry erosion in complex flows: Experiment and CFD"*, Seventh International Conference on CFD in the Minerals and Process Industries, Melbourne, Australia.

LAUNDER, B.E. and SPALDING, D.B., (1974), "The numerical computation of turbulent flows", *Computer methods in applied mechanics and engineering* **3**: 269-289.

LAUNDER, D.E. and SHARMA, B.T., (1977), "Application of the Energy Dissipation Model of Turbulence to the Calculation of Flow near a Spinning Disc", *Letters in Heat and Mass Transfer* **1**(2): 131-138.

LESTER, D.R., GRAHAM, L.A. and WU, J., (2010), "High precision suspension erosion modeling", *Wear* **269**(5-6): 449-457.

SOLNORDAL, C.B. and WONG, C.Y., (2011). *"Application of a Combined CFD/Experimental Approach to Quantifying Erosion Rate"*, CFD2011 - 8th International Conference on Computational Fluid Dynamics in the Oil & Gas, Metallurgical and Process Industries, Trondheim, Norway.

WONG, C.Y., SOLNORDAL, C., SWALLOW, A., WANG, S., GRAHAM, L. and WU, J., (2012), "Predicting the material loss around a hole due to sand erosion", *Wear* **276-277**: 1-15.

